FGF signaling facilitates postinjury recovery of mouse hematopoietic system

*Meng Zhao,[1] *Jason T. Ross,[1,2] Tomer Itkin,[3] John M. Perry,[1] Aparna Venkatraman,[1,4] Jeffrey S. Haug,[1] Mark J. Hembree,[1] Chu-Xia Deng,[5] Tsvee Lapidot,[3] Xi C. He,[1] and Linheng Li[1,2]

[1]Stowers Institute for Medical Research, Kansas City, MO; [2]Department of Pathology and Laboratory Medicine, University of Kansas Medical Center, Kansas City, KS; [3]Department of Immunology, Weizmann Institute of Science, Rehovot, Israel; [4]Centre for Stem Cell Research, Christian Medical College, Vellore, India; and [5]National Institute of Diabetes and Digestive and Kidney Diseases, National Institutes of Health, Bethesda, MD

Previous studies have shown that fibroblast growth factor (FGF) signaling promotes hematopoietic stem and progenitor cell (HSPC) expansion in vitro. However, it is unknown whether FGF promotes HSPC expansion in vivo. Here we examined FGF receptor 1 (FGFR1) expression and investigated its in vivo function in HSPCs. Conditional knockout (CKO) of *Fgfr1* did not affect phenotypical number of HSPCs and homeostatic hematopoiesis, but led to a reduced engraftment only in the secondary transplantation. When treated with 5-fluorouracil (5FU), the *Fgfr1* CKO mice showed defects in both proliferation and subsequent mobilization of HSPCs. We identified megakaryocytes (Mks) as a major resource for FGF production, and further discovered a novel mechanism by which Mks underwent FGF-FGFR signaling dependent expansion to accelerate rapid FGF production under stress. Within HSPCs, we observed an up-regulation of nuclear factor κB and CXCR4, a receptor for the chemoattractant SDF-1, in response to bone marrow damage only in control but not in *Fgfr1* CKO model, accounting for the corresponding defects in proliferation and migration of HSPCs. This study provides the first in vivo evidence that FGF signaling facilitates postinjury recovery of the mouse hematopoietic system by promoting proliferation and facilitating mobilization of HSPCs. (*Blood*. 2012; 120(9):1831-1842)

Introduction

Fibroblast growth factors (FGFs) are a large group of secreted molecules that regulate cell migration, proliferation, and differentiation in both embryonic and adult development.[1,2] FGFs mediate their cellular responses by binding to and activating a family of 4 receptor tyrosine kinases designated as the FGF-receptors FGFR1 through FGFR4, which display different ligand-binding characteristics and biologic functions.[3] FGF signaling is important for hematopoietic developmental regulation,[4,5] and FGFR1 was shown to be preferentially expressed in adult hematopoietic stem and progenitor cells (HSPCs).[6] Although FGF ligands support HSPC expansion in vitro,[7,8] the role of FGF signaling via FGFR1 in vivo has not been elucidated.

Treatment with chemotherapeutic drugs, such as cyclophosphamide and 5-fluorouracil (5FU),[9,10] induces a multistep bone marrow (BM) stress response: (1) actively cycling cells are eliminated, including cycling HSPCs[9,10]; (2) surviving quiescent long-term hematopoietic stem cells (LT-HSCs) are subsequently activated to expand; (3) some expanded HSCs give rise to short-term HSCs (ST-HSCs) for further proliferation; and (4) some HSPCs egress from BM to the blood circulation and extramedullary sites, such as spleen (ie, mobilization), to further proliferate and differentiate.[11-13] In homeostatic hematopoiesis, HSPCs are primarily localized within BM where they associate with niches that regulate their activity.[14-18] Although a small percentage of HSPCs routinely circulate from BM to peripheral blood (PB) and home back to BM,[19,20] the number of HSPCs that migrate from BM can be markedly increased by certain stimuli during mobilization.[21-25] These stimuli include tissue damaging chemotherapeutic drugs as previously mentioned and various cell signaling molecules, such as stromal derived factor-1 (SDF-1)[26] and AMD3100, a small molecule that interferes with the interaction between SDF-1 and its receptor CXCR4.[27]

In this report, we used 3 conditional knockout (CKO) mouse models: *Mx1-Cre*, *Scl-Cre-ER^T* (hereafter referred to as *Scl-Cre*), and *Tek-Cre* (or *Tie2-Cre*) to study the role of FGFR1 in HSPCs. Although each model has its own advantage and disadvantage, the results from testing FGFR1 in all 3 models support a critical role of FGFR1 signaling in promoting proliferation and facilitating mobilization of HSPCs as an essential process of hematopoietic recovery in response to BM damage.

Methods

Animals and treatment protocol

Fgfr1$^{fx/fx}$ mice[28] were mated with *Mx1-Cre*,[29] *Scl-Cre*,[30] or *Tek-Cre*[31] lines to generate *Mx1-Cre:Fgfr1$^{fx/fx}$*, *Scl-Cre:Fgfr1$^{fx/fx}$*, or *Tek-Cre:Fgfr1$^{fx/fx}$ Fgfr1* CKO lines, respectively. All mice were backcrossed with C57Bl/6 to achieve the C57Bl/6 background. Genotyping was performed on tail biopsies using a polymerase chain reaction (PCR)–based method developed by Transnetyx (Cordova). To induce gene deletion, polyinosinic: polycytidylic acid (pIpC; GE Healthcare) was injected intraperitoneally every other day at a dose of 250 μg per injection to *Mx1-Cre:Fgfr1$^{fx/fx}$* mice for a total of 7 injections, or tamoxifen (TMX; Sigma-Aldrich) was injected intraperitoneally every day at a dose of 2 mg per injection to *Scl-Cre:Fgfr1$^{fx/fx}$* mice for 5 days. Mice received 5FU or AMD3100 treatment only after 2 to 3 weeks following completion of induction for gene-deletion.

Submitted November 29, 2011; accepted July 8, 2012. Prepublished online as *Blood* First Edition paper, July 16, 2012; DOI 10.1182/blood-2011-11-393991.

*M.Z. and J.T.R contributed equally to this work.

The online version of this article contains a data supplement.

The publication costs of this article were defrayed in part by page charge payment. Therefore, and solely to indicate this fact, this article is hereby marked "advertisement" in accordance with 18 USC section 1734.

FVB/N and FVB/N *Fgf2* knockout mice were as described.[32] The adult mice were defined as beyond 2 months old. All mice used in this study were housed in the animal facility at the Stowers Institute for Medical Research (SIMR) and handled according to SIMR and National Institutes of Health (NIH) guidelines. Mice were treated with reagents as follows: injected once via tail vein with 5FU (Sigma-Aldrich) at 150 μg/g body weight (BW),[33] injected once subcutaneously with AMD3100 (Sigma-Aldrich) at 5 μg/g BW.[27] PB, BM, and/or spleen tissue was harvested at various time points after 5FU treatment, and 60 minutes after AMD3100 treatment. All procedures were approved by the Institutional Animal Care and Use Committee of SIMR.

Flow cytometry analysis of hematopoietic cells

Hematopoietic cells were harvested from spleen, PB, and BM of the femurs and tibias. The flow analysis for HSCs was previously described.[34,35] Megakaryocytes (Mks) were identified by their large size (forward scatter high, FSC^{hi}) combined with staining with a monoclonal antibody to CD41 (eBioscience). For detection of FGFR1 and FGF2 expression in Mks, total BM cells were incubated with rat anti CD41-PE (eBioscience) and with rabbit anti-FGFR1 (Abcam) antibodies followed by incubation with 2nd 488 anti–rabbit (Jackson ImmunoResearch Laboratories) or cells were stained with rat anti–CD41-PE and permeabilized using BD Perm/Fix kit (BD Biosciences) according to the manufacturer's protocol, and then incubated with biotinylated anti-FGF1 (Peprotech) antibody followed by incubation with streptavidin-APC (Biolegend). Gating on FSC^{hi} $CD41^{+}$ cell population that enriches Mks, we measured the mean fluorescence intensity (MFI) as the levels of FGFR1 or FGF1. Cell viability was tested by annexin V (Invitrogen) and 7-AAD (Invitrogen). Cell sorting and analysis were done on the Cyan ADP (Dako), MoFlo (Dako), and/or Influx (BD Biosciences). Data analysis was performed using FlowJo Version 7.6.4 software.

Transplantation assays

Transplantation experiments were performed with BM, spleen or PB cells from donor mice (CD45.2) that had received either none or with 5FU 12 days prior. Two $\times 10^5$ competitor/rescue whole Ptprc BM cells (CD45.1) were transplanted into each lethally irradiated (10 Gy) Ptprc (CD45.1) recipient with indicated numbers of donor cells. Repopulation was measured every 4 weeks after transplantation by collection of PB, red blood cell lysis, and staining of CD45.1 (recipient) versus CD45.2 (donor) engraftment.

Quantitative real-time RT-PCR and RNA-sequencing analysis

Total RNA was isolated using TRIzol (Invitrogen) according to the manufacturer's protocol. Real-time reverse transcription (RT)–PCR reactions were performed in triplicate using the Quantitect SYBR Green RT-PCR kit (QIAGEN) on an iQ5 RT-PCR detection system (Bio-Rad Laboratories) or ABI 7900 (Applied Biosystems) according to the manufacturer's instructions. The RNA-sequencing library was prepared using illumina TruSeq RNA sample prep kit (no. FC-122-1001). A total of 10 fmol library fragments were loaded to cBot to generate clusters, followed by sequencing on an Illumina HiSeq 2000. Gene expression was quantitated using Cufflinks 1.0.3. For details please see supplemental Methods (available on the *Blood* Web site; see the Supplemental Materials link at the top of the online article).

Genotyping

DNA was purified from targeted cells using QIAamp DNA blood kit (QIAGEN) and PCR was performed using primers, *Fgfr1* a, *Fgfr1* c for recombined allele, and *Fgfr1* b, *Fgfr1* c for unrecombined allele. Sequences for primers *Fgfr1* a, b, and c are 5′gtattgctggcccactgttc3′, 5′ctggtatcctgtgcctatc3′ and 5′caatctgatcccaagaccac3′, respectively.

Cell migration assays

Cell migration was studied using 6.5 mm, 5 μm pore size transwell inserts in 24-well cluster plates (Corning-Costar). Five-thousand $lineage^{-}Sca\text{-}1^{+}c\text{-}Kit^{+}$ (LSK) cells were flow sorted into 0.1 mL Dulbecco modified Eagle medium (DMEM) supplemented with 5% horse serum in the upper chamber. Chemotaxis toward 100 ng/mL murine CXCL12/SDF-1α (R&D Systems) in 0.6 mL DMEM + 5% HS in the lower chamber was allowed to continue for 4 hours at 37°C and 5% CO_2. Cells that had migrated to the lower chamber were visualized and enumerated using a Leica DM IL (Leica Microsystems). Where indicated, 100 ng/mL FGF1or FGF2 (R&D Systems) and the following chemical inhibitors were included in the media of both the upper and lower chambers: SU5402 at 25μM (Calbiochem), LY294002 at 50μM (BIOMOL Research Laboratories), and PD98059 at 50μM (Sigma-Aldrich).

Cell culture

$Flk2^{-}$LSK cells, LSK cells, or total BM cells were sorted into 96-well U-bottom tissue culture plates at 500 $Flk2^{-}$LSK cells, 600 LSK cells or 1 to 2×10^5 BM cells/well with 180μL media/well. Cells were incubated at 37°C, 5% O_2, 5% CO_2 (balance N_2). Defined HSC expansion media was based on previous reports,[36] which included StemSpan serum-free expansion medium (SFEM; StemCell Technologies) supplemented with 10 mg/mL heparin (Sigma-Aldrich), 10 ng/mL recombinant mouse stem cell factor (Biovision), and 20 ng/mL Tpo (Cell Sciences). Where indicated, the chemical inhibitor SU5402 (Calbiochem) or nuclear factor (NF)κB inhibitor (EMD Biosciences) was added to the culture media at 1 or 5μM. FGF1, FGF2, FGF4, and FGF10 (R&D Systems) were added at 50 ng/mL to the culture media, respectively, for 2 weeks.

Immunohistochemistry and immunostaining

Tissues collected for immunohistochemistry were fixed in unbuffered zinc formalin (Richard-Allan Scientific) for 24 hours at room temperature. Femurs and tibias were decalcified in Immunocal (Decal Chemical) for 24 hours at room temperature. Tissues were embedded in paraffin and 3μM sections were obtained. Tissues were stained with a rabbit polyclonal antibody to von Willibrand factor (VWF; AbCam) at a dilution of 1:300. Secondary staining was done with the EnVision+ System-HRP Labeled anti–rabbit polymer (Dako). For single-cell staining, cells were sorted onto poly-lysine coated slides, fixed with methanol and stained for NFκB P65 (Cell Signaling Technology) using 1:200 dilution. Images were taken on an Axiomager Z1 (Zeiss) with AxioVision 4.7.2.0.

Enzyme-linked immunosorbent assays

For the FGF1, FGF2, and SDF-1 detection, a monoclonal antibody to FGF1 (PeproTech), FGF2 (R&D Systems), or SDF-1 monoclonal antibody 79018 (R&D Systems) was used for capture, and biotinylated antibodies FGF1 (PeproTech), FGF2 (R&D Systems), or biotinylated anti–SDF-1 (R&D Systems) were used for detection using streptavidin-horseradish peroxidase. Plates were read with an enzyme-linked immunosorbent assay (ELISA) reader and analyzed according to the standard curve and Bradford assay results. The standard curve was made using recombinant mouse FGF1, FGF2 (PeproTech), or hSDF-1 (R&D Systems).

Colony forming unit assays

In vitro colony forming unit (CFU) assays detected a mixture of myeloid progenitors including: erythroid (BFU-E), granulocyte-macrophage (CFU-G, CFU-M, and CFU-GM), and multipotential granulocyte, erythroid, macrophage, and Mk (CFU-GEMM). The assay was performed using 2×10^5 PB cells per well of a 12-well tissue culture plate (Becton Dickinson) and 0.9 mL MethoCult GF M3434 Media (StemCell Technologies) following the manufacturer's instructions. Colonies were evaluated and counted on day 12 of culture using a Leica DM IL microscope (Leica Microsystems).

CFU-Mk assays

Mk progenitor assay was performed on BM cells using MegaCult-C media (StemCell Technologies) supplemented with 50 ng/mL rmTpo, 20 ng/mL

rmIL-6, and 10 ng/mL rmIL-3. CFU-Mks were stained for acetylcholinesterase activity and scored after 7 days incubation according to the manufacturer's protocol.

Statistical analysis

Data were expressed as mean ± SD. Pairwise comparisons were performed using the Student *t* test.

Results

FGFR1-mediated signaling is dispensable for homeostatic hematopoiesis but important for BM recovery under stress

To investigate the function of FGF signaling in HSPCs, we induced *Mx1-Cre:Fgfr1*$^{fx/fx}$ control and CKO mice for gene inactivation. After a recovery period of 3 weeks, *Mx1-Cre*$^{+}$*:Fgfr1*$^{fx/fx}$ mice exhibited normal hematopoiesis compared with *Mx1-Cre*$^{-}$*:Fgfr1*$^{fx/fx}$ controls, as indicated by similar numbers of HSPCs (LSK cells) in BM, as well as normal levels of mature myeloid and lymphoid lineages in PB, spleen, and thymus (supplemental Figure 1). Because pIpC used for induction of *Mx1-Cre* can cause HSPC proliferation independent of FGF signaling and *Scl-Cre* has lower recombination efficiency, we used the *Tek-Cre* induced *Fgfr1* CKO model to conduct the repopulation assay. We demonstrated that *Fgfr1* CKO did not significantly affect HSPC numbers and function in primary transplantation but did influence HSPC repopulation after secondary transplantation (supplemental Figures 2-3). These results indicate that loss of FGF signaling via FGFR1 does not impact homeostatic hematopoiesis but can compromise HSC function when multiple rounds of expansion are required.

Although not required for homeostasis, FGF signaling was previously reported to be involved in neonatal motor cortex injury recovery.[37] We asked whether FGF signaling is involved in BM stress response. As a cytotoxic agent, 5FU initiated BM stress response by killing actively cycling cells, including cycling HSPCs,[9,10] causing the number of LSK cells in BM to decline within the first week after 5FU treatment (Figure 1A). Extensive cell death led to activation of surviving HSCs, followed by proliferation of LT-HSCs, ST-HSCs, and multipotent progenitor cells (MPPs; all contained in LSK cells) from day 7 through day 12 after 5FU.[38] We observed that *Mx1-Cre*$^{-}$*:Fgfr1*$^{fx/fx}$ and *Mx1-Cre*$^{+}$*:Fgfr1*$^{fx/fx}$ mice showed similar nadirs of LSKs between days 5 and 7 after 5FU (Figure 1A). Whereas LSKs in BM of *Mx1-Cre*$^{-}$*:Fgfr1*$^{fx/fx}$ mice expanded dramatically on days 10 and 12 after 5FU, LSK expansion in *Mx1-Cre*$^{+}$*:Fgfr1*$^{fx/fx}$ mice was significantly impaired (Figure 1A). Because the *Mx-1* promoter-driving Cre expression is in hematopoietic cells as well as in stromal cells,[29] we also used a TMX-induced HSPC specific *Scl-Cre* mouse line,[30] and a hematopoietic and endothelial specific *Tek-Cre* line to determine whether FGFR1 is required for HSPC recovery after 5FU treatment or whether it acts indirectly on HSPCs through nonhematopoietic stromal components. For this purpose, we compared the pIpC-induced *Mx1-Cre*, TMX-induced *Scl-Cre,* and *Tek-Cre*–mediated *Fgfr1* CKO models. After Cre induction, mice were treated with 5FU (Figure 1B). Twelve days after 5FU, when the largest difference between controls and *Fgfr1* CKO models was observed (Figure 1A), all 3 *Fgfr1* CKO models had decreased frequency and absolute number of LSK cells in BM compared with littermate controls (37%, 66.5%, and 57.2% decrease, respectively in *Mx1-Cre*, *Scl-Cre, Tek-Cre*; Figure 1C). In response to 5FU-induced BM damage, surviving LSK cells undergo mobilization and significant expansion as seen in spleen of control mice; however, we observed substantially fewer LSK cells in the spleens of *Fgfr1* CKO mice (95.6%, 98%, and 90.45% decrease, respectively in *Mx1-Cre*, *Scl-Cre*, and *Tek-Cre*; Figure 1D). We also noticed the extent of HSPC increase in the *Cre*$^{-}$ control group was greater with pIpC induction (5.8×10^5 in BM, 2.4×10^6 in spleen) than with TMX induction (1.7×10^5 in BM, 7.1×10^5 in spleen), and greater than in the noninduced *Tek-Cre* model (2.2×10^5 in BM, 1.4×10^6 in spleen; Figure 1C-D). This discrepancy can be explained, at least in part, by the added effect of interferon (IFN) induced by pIpC.[39] These results indicate that FGFR1 promotes HSPC proliferation and potential migration during BM recovery in response to BM damage.

Given the potential side effect from pIpC in *Mx1-Cre* model, we further verified our finding by performing whole BM transplantations from *Scl-Cre*$^{-}$*:Fgfr1*$^{fx/fx}$ and *Scl-Cre*$^{+}$*:Fgfr1*$^{fx/fx}$ donors into lethally irradiated recipients (supplemental Figure 4). We found that the BM cells from *Scl-Cre*$^{+}$*:Fgfr1*$^{fx/fx}$ exhibited lower short-term engraftment at 4 weeks but recovered at 12 and 16 weeks compared with control donors. To exclude the potential cytotoxicity caused by Cre-ER^{T}, we tested the *Scl-Cre*$^{+}$*:Fgfr1*$^{+/+}$ control mice after TMX induction and 5FU treatment, and this resulted in normal HSPC recovery (supplemental Figure 5). Because the HSPCs that escaped Cre-induced *Fgfr1* excision could potentially contribute to long-term repopulation, we measured recombination efficiency and found that both *Mx1-Cre* and *Tek-Cre* models resulted in complete excision in both the LSK and lineage-positive (mature cells) populations; the *Scl-Cre* model, however, revealed incomplete recombination (~ 50%) in both populations (Figure 2A). The gene inactivation efficiencies in LSK populations were confirmed by qRT-PCR (Figure 2A).The mRNA levels of *Fgfr1* in both *Mx1-Cre*$^{+}$*:Fgfr1*$^{fx/fx}$ and *Tek-Cre*$^{+}$*:Fgfr1*$^{fx/fx}$ were largely reduced; however, *Scl-Cre*$^{+}$*:Fgfr1*$^{fx/fx}$ showed only a 50% reduction compared with littermate controls. In addition, we noticed a 44% and 41% increase of *Fgfr3*, respectively, in *Mx1-Cre*$^{+}$*:Fgfr1*$^{fx/fx}$ and *Tek-Cre*$^{+}$*:Fgfr1*$^{fx/fx}$ mice compared with littermate controls. This suggested a potential compensation from FGFR3 when FGFR1 was inactivated. However, *Fgfr1* CKO still adversely affected after BM damage recovery of HSPCs (Figure 1), which indicated an influence from FGFR3 compensation for BM recovery is not sufficient.

To prove the decrease of functional HSPCs in *Fgfr1* CKO mice after BM damage, we conducted a competitive repopulation assay using the *Tek-Cre* CKO model that has high recombination efficiency (Figure 2A) and no side effect from pIpC. First, we observed, in *Fgfr1* CKO mice at 12 days after 5FU treatment, that the frequency and absolute number of HSPCs decreased in BM (56.1% for LT-HSCs, 41.5% for ST-HSCs, and 61.5% for MPPs; Figure 2B-C) and in spleen (73.3% for LT-HSCs, 87.8% for ST-HSCs, and 87.6% for MPPs; Figure 2E-F). Next, we transplanted equal number of BM or spleen cells isolated from *Tek-Cre*$^{-}$*:Fgfr1*$^{fx/fx}$ and *Tek-Cre*$^{+}$*:Fgfr1*$^{fx/fx}$ mice at 12 days after 5FU with rescue cells into lethally irradiated recipients. We observed that BM cells and spleen cells from *Tek-Cre*$^{+}$*:Fgfr1*$^{fx/fx}$ mice resulted in lower engraftment than those from *Tek-Cre*$^{-}$*:Fgfr1*$^{fx/fx}$ (Figure 2D-G; 26% decrease in BM cells and 48% decrease in spleen cells, respectively, at 16 weeks posttransplantation). These data demonstrate that the numbers of functional HSPCs in BM and spleen of *Fgfr1* CKO mice are indeed reduced after BM damage, supporting the functional requirement of FGFR1 for HSPCs during BM recovery.

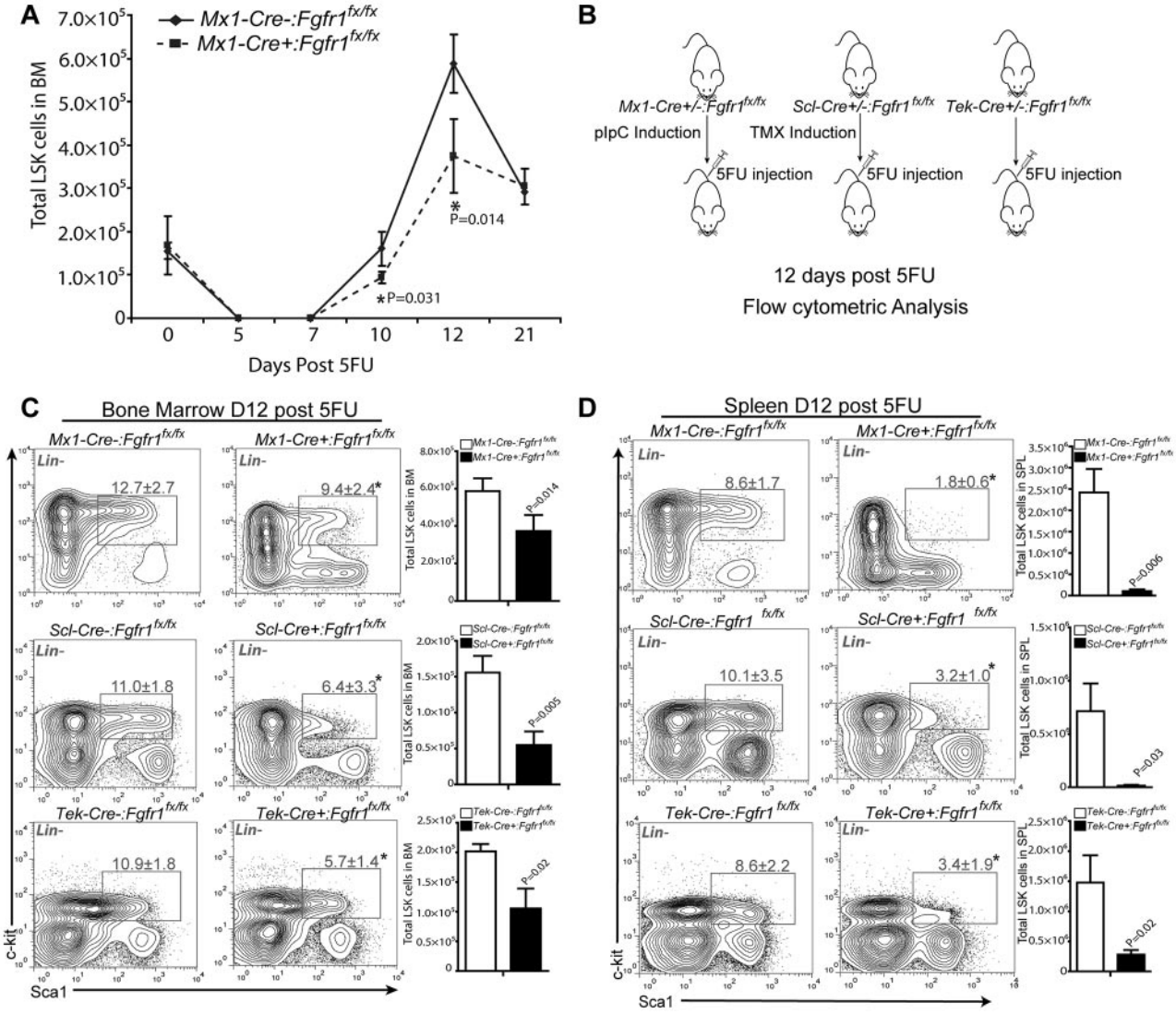

Figure 1. FGFR1 inactivation impairs HSPC recovery after BM damage. (A) Comparison of LSK numbers in BM of *Mx1:Control* and *Mx1:CKO* mice at the indicated times after 5FU (n = 2-4). (B) Illustration of Cre induction, 5FU-induced BM damage, and analyses of *Fgfr1* control (*Cre*$^{-}$*:Fgfr1*$^{fx/fx}$) and CKO (*Cre*$^{+}$*:Fgfr1*$^{fx/fx}$) mice. Polyinosinic:polycytidylic acid (pIpC). Tamoxifen (TMX). (C) Flow cytometric analyses of the LSK population and comparison of absolute numbers of LSK cells in BM from *Mx1:Control*, *Mx1:CKO* (n = 4), *Scl:Control*, *Scl:CKO* (n = 6), and *Tek:Control*, *Tek:CKO* (n = 6) mice 12 days after 5FU. (D) Flow cytometric analyses of the LSK population and comparison of absolute numbers of LSK cells in spleen from *Mx1:Control*, *Mx1:CKO* (n = 4), *Scl:Control*, *Scl:CKO* (n = 5), and *Tek:Control*, *Tek:CKO* (n = 6) mice 12 days after 5FU (*$P < .05$). Data pooled from at least 2 independent experiments.

FGF-FGFR1 signaling is activated by 5FU treatment

Because we observed that FGFR1 is dispensable for homeostatic hematopoiesis but important for BM recovery under stress, we examined whether FGF-FGFR1 signaling is activated under stress. First, we performed an RNA-sequencing analysis to examine the expression of *Fgfrs* in HSPCs. Among the 4 *Fgfrs*, we detected *Fgfr1* and *Fgfr3* expressions in LT-HSCs, ST-HSCs, and MPPs, with *Fgfr1* expressing higher than *Fgfr3* (Figure 3A). We then compared expressions of *Fgfrs* under stressed conditions. BM CD34^{-}LSK (enriched for LT-HSCs) cells were harvested from untreated and 5FU-treated wild-type (WT; C57Bl/6) mice, and expressions of *Fgfrs* were measured by qRT-PCR. At day 5 after 5FU, we observed that only *Fgfr1* had a significant increase (2-fold), supporting the role of FGFR1-mediated signaling in promoting HSPC proliferation after stress (Figure 3B). Next, we compared expression levels of FGF ligands specific for FGFR1 (FGF1, 2, 3, 4, 5, and 10) in BM of C57/B6 mice under normal and 5FU-induced stress conditions.[1] Five days after 5FU, the mRNA levels of *Fgf1*, *Fgf2*, *Fgf5*, and *Fgf10* showed significant increase, with *Fgf1* displaying the highest increase (12, 2.6, 2.3, and 4.7-fold, respectively; Figure 3C). In addition, the protein levels of FGF1 and FGF2 in BM increased 1.7-fold and 1.5-fold, respectively after 5FU, as measured by ELISAs (Figure 3D). These data suggest that FGF1, FGF2, FGF5, and FGF10 are probably the signals promoting HSPC proliferation in response to stress, which is consistent with published studies using FGF1 and FGF2 to expand HSPCs in vitro.[7,8]

FGF signaling drives HSPC expansion in vitro

To further test whether FGF signaling via FGFR1 plays a role in HSPC expansion, we conducted an in vitro culture experiment using a previously reported method, in which the functional HSCs are maintained.[35,36] BM Flk2^{-}LSKs (enriched with both LT and ST-HSCs) from *Mx1-Cre*$^{-}$*:Fgfr1*$^{fx/fx}$ and *Mx1-Cre*$^{+}$*:Fgfr1*$^{fx/fx}$ mice were sorted and used for in vitro culture. After 2 weeks culture, we

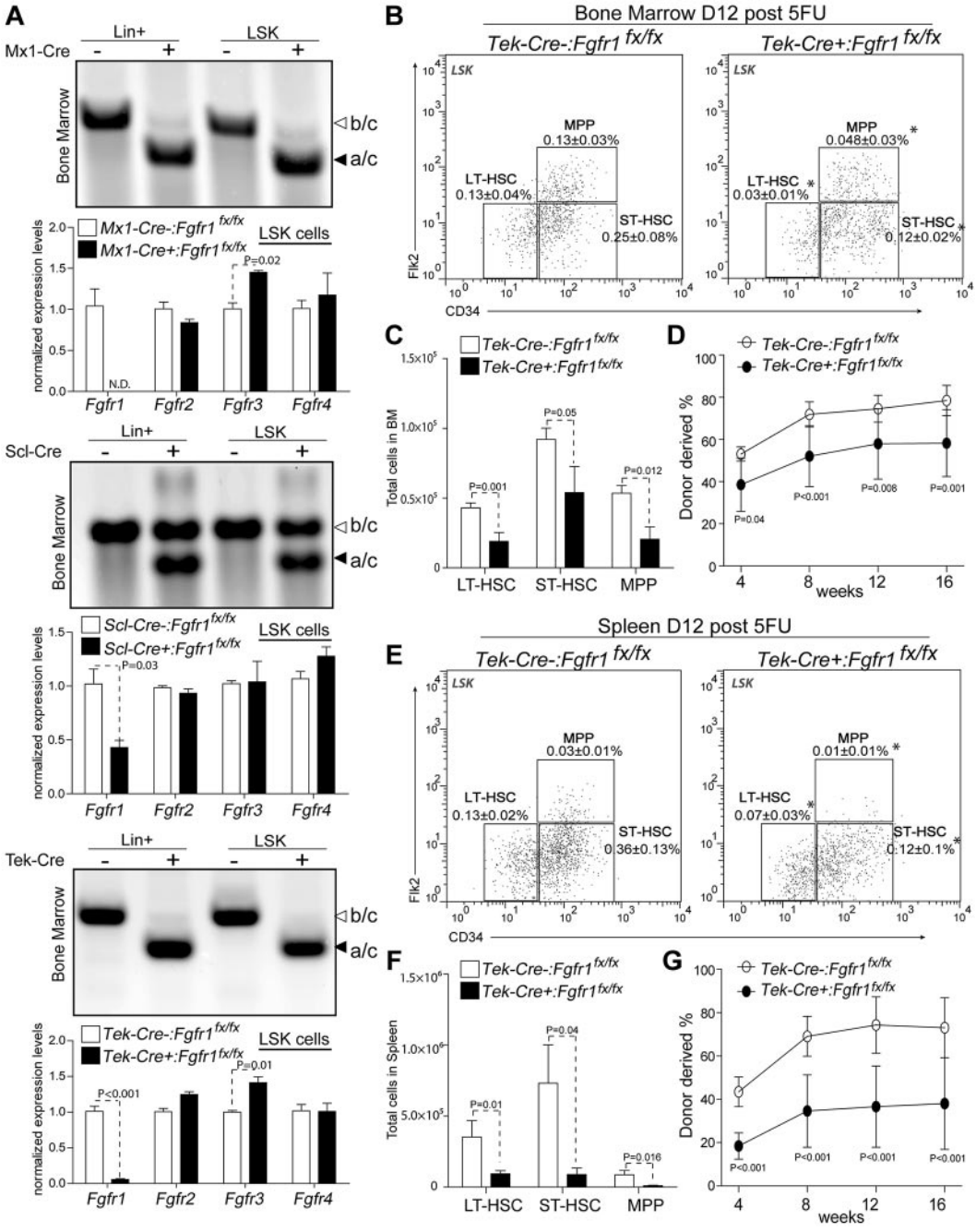

Figure 2. Comparison of gene deletion efficiency in *Fgfr1* CKO models and testing functions of HSPCs in BM and spleen after BM damage. (A) Purified DNA and mRNA from sorted lineage positive (Lin$^+$) and LSK populations in BM of *Fgfr1* control and *Fgfr1* CKO animals at 12 days after 5FU. PCR to detect recombined (primer a/c 300 bp) and unrecombined allay (primer b/c 400 bp). qRT-PCR detection of gene expression analysis of *Fgfr1, 2, 3, 4* in LSK cells. ND = not detected. (B-E) Flow cytometric analyses of HSPCs (LT-HSC, ST-HSC, MPP) in LSK population in BM (B) and spleen (E) of *Tek:Control*, *Tek:CKO* (n = 4-6) mice 12 days after 5FU. Frequencies of total TNC shown in plots. (C-F) Comparison of absolute numbers of HSPCs (LT-HSC, ST-HSC, MPP) in BM (C) and spleen (F) from *Tek:Control*, *Tek:CKO* (n = 4-6) mice 12 days after 5FU. (D-G) Two $\times$ 10^5 BM cells (D) or 2.5 $\times$ 10^5 spleen cells (G) from *Tek:Control, Tek:CKO* mice (CD45.2) transplanted 12 days after 5FU with 2 $\times$ 10^5 rescue BM cells (CD45.1) into lethally irradiated Ptprc recipients. PB analysis for total engrafted donor cells at 4, 8, 12 and 16 weeks posttransplantation (n = 10 per group). Error bars indicate SD (*$P < .05$).

found that BM Flk2$^-$LSKs from *Mx1-Cre$^-$:Fgfr1$^{fx/fx}$* mice expanded much more robustly (by 10.1-fold) than those from *Mx1-Cre$^+$:Fgfr1$^{fx/fx}$* mice (Figure 4A-B). Furthermore, the FGFR inhibitor SU5402 blocked expansion of WT Flk2$^-$LSKs in vitro 3.2-fold at 1μM and 11-fold at 5μM (Figure 4B). These in vitro data confirm the importance of FGFR1 signaling in facilitating the expansion of HSPCs.

To distinguish direct and indirect influence of FGFs in this regard, we performed in vitro experiments to culture mixed BM cells or sorted LSK cells. Total BM cells harvested from *Scl-Cre$^-$:Fgfr1$^{fx/fx}$* and *Scl-Cre$^+$:Fgfr1$^{fx/fx}$* mice were cocultured with different FGF ligands for 2 weeks. BM cells cultured with FGF1 or FGF2 expanded CD34$^-$LSK cells 2 times greater than without FGF1 or FGF2 (Figure 4C). This result is consistent with a previous report.[8] FGF4 and FGF10 did not expand HSPCs. When we conducted this culture with sorted LSK cells, we surprisingly found that only FGF1 expanded HSPCs 3 times greater than without FGF1, but not with FGF2, and also that FGF4 instead of

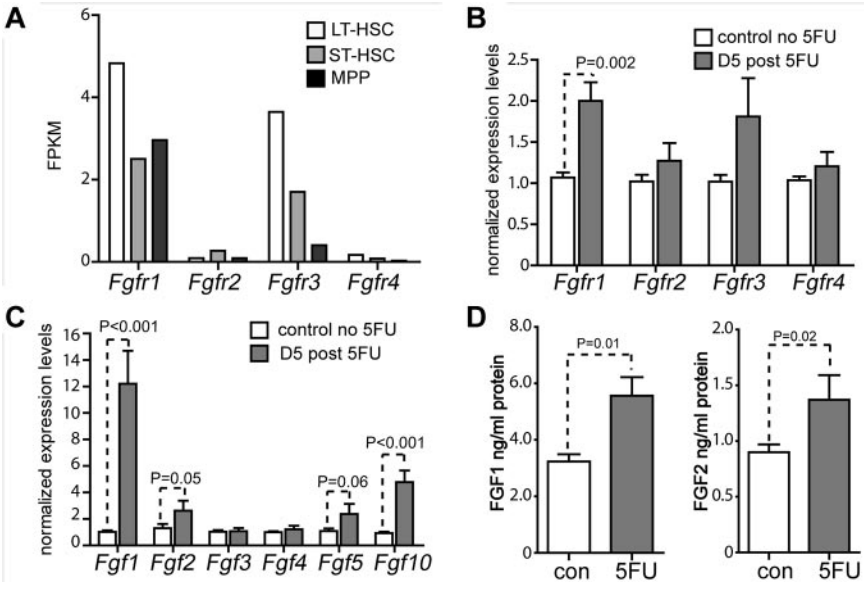

Figure 3. FGF signal is activated post BM damage. (A) RNA-seq analysis of HSPCs for *Fgfrs*. Expression level shown by FPKM (fragments per kilobase of exon per million fragments mapped). (B) Gene expression analysis of *Fgfr1, 2, 3, 4* using qRT-PCR on BM CD34$^-$LSK cells from C57Bl/6 WT mice 5 days after 5FU (n = 3). (C) Gene expression analysis of *Fgf1, 2, 3, 4,* and *10* using qRT-PCR on BM cells from C57Bl/6 WT mice on the days indicated after 5FU (n = 3). (D) FGF1 and FGF2 protein levels as determined by ELISA of BM supernatants of C57Bl/6 WT mice after 5FU at 5 and 10 days, respectively (n = 3).

FGF10 slightly expanded HSPCs (Figure 4C). This result suggests that FGF1 more directly regulates HSPCs, whereas FGF2 may indirectly influence HSPCs by regulating other types of BM cells.

Mechanistically, we noted by measuring with qRT-PCR that the FGFR1 downstream target NFκB, a known HSC survival factor, showed an up-regulation in Flk2$^-$LSK cells from *Mx1-Cre$^-$:Fgfr1$^{fx/fx}$* mice but not from *Mx1-Cre$^+$:Fgfr1$^{fx/fx}$* mice on day 5 (3.9-fold) and day 10 (5.4-fold) after 5FU treatment (Figure 4D). As the NFκB activity is associated with its nuclear translocalization (the p65 form), we compared NFκB p65 in CD34$^-$LSK cells isolated from *Scl-Cre$^-$:Fgfr1$^{fx/fx}$* and *Scl-Cre$^+$:Fgfr1$^{fx/fx}$* mice using immunostaining. We found that NFκB was more abundant in the nucleus of CD34$^-$LSK cells from *Scl-Cre$^-$:Fgfr1$^{fx/fx}$* mice (42%) than from *Scl-Cre$^+$:Fgfr1$^{fx/fx}$* mice (23%) at 12 days after 5FU (Figure 4E). We further examined whether NFκB pathway is functionally required for HSPC expansion in vitro. We found that in mixed BM cell culture, NFκB inhibitor (at 1μM and 5μM, respectively) reduced the expansion of CD34$^-$LSKs in vitro without FGF (43% and 54%), with FGF1 (45% and 60%), or with FGF2 (36% and 84%; Figure 4F). Taken together, these data further support the conclusion that FGF1 and FGF2 signaling, mediated mainly by FGFR1 and potentially other receptors, such as FGFR3, are important for HSPC expansion, at least phenotypically, in response to BM damage.

FGFR1 inactivation reduces the number of megakaryocytes and the associated up-regulation of FGF induced by 5FU treatment

As observed in our previous report, HSPCs were surrounded by Mks[35] at 2 weeks post culture as shown by cytospin and hematoxylin and eosin (H&E) staining (Figure 5A). We further measured the frequency and number of Mks post culture by analyzing FSC^{hi}CD41$^+$ cells.[40] The frequency of Mks initially was 3.4% but increased to 71.8% post culture, and the absolute number increased 20.6-fold (Figure 5A), suggesting that Mks may play a role in supporting HSPC expansion. Consistent with this observation, Mks have been reported to migrate to the endosteum in response to irradiation-induced BM damage to facilitate recovery and expansion of the osteoblastic niche, which in turn promotes HSC expansion.[41] Next, we examined Mks response to 5FU-induced BM damage in C57Bl/6 BM in vivo. The frequency of Mks (FSC^{hi}CD41$^+$) increased from 3.4% in BM in steady-state (no 5FU) to 7.8% in BM at 5 days after 5FU (Figure 5B). We also found that Mks (FSC^{hi}CD41$^+$) in steady-state had relatively higher *Fgfr1* levels (2.1-fold) than non-Mks (non-FSC^{hi}CD41$^+$ cells). Strikingly, on day 5 after 5FU, *Fgfr1* levels increased much more significantly in Mks (56.5-fold) than in non-Mks cells (16-fold; Figure 5B).

Because our results indicate that Mk expansion after 5FU is correlated with FGFR1 up-regulation, we therefore analyzed Mks stained by VWF in *Mx1-Cre$^-$:Fgfr1$^{fx/fx}$* and *Mx1-Cre$^+$:Fgfr1$^{fx/fx}$* BM 10 days after 5FU treatment. Quantification of VWF$^+$ Mks showed that 5FU induced a significant increase (4.3-fold) in the number of Mks in BM compared with control mice (Figure 5C). Intriguingly, the number of Mks in BM from *Mx1-Cre$^+$:Fgfr1$^{fx/fx}$* mice was 51.7% less than from *Mx1-Cre$^-$:Fgfr1$^{fx/fx}$* mice (Figure 5C). In addition, using functional CFU-Mk assays, we found significantly fewer CFU-Mk colonies (54.8% less) in *Scl-Cre$^+$:Fgfr1$^{fx/fx}$* BM 12 days after 5FU than in *Scl-Cre$^-$:Fgfr1$^{fx/fx}$* BM (Figure 5D). In addition, we noticed that Mks were attracted to the perivascular area after 5FU treatment, and this aggregation was much reduced in *Fgfr1* CKO mice (Figure 5E). This is consistent with a previous report that FGF signaling is involved in Mk recovery after myelosuppression, in which FGF4-enhanced Mk progenitor localization to the vascular niche, survival, and maturation.[42]

These observations raised the possibility that Mks are a major resource of FGF production and that Mks may themselves respond to FGF signals. To test whether Mks secrete FGFs that might support HSPC expansion under 5FU-induced stress, we measured FGFs in sorted Mks (FSC^{hi}CD41$^+$) from *Scl-Cre$^-$:Fgfr1$^{fx/fx}$* and *Scl-Cre$^+$:Fgfr1$^{fx/fx}$* BM. *Fgf1*, *Fgf2*, and *Fgf10* expressions were increased (2.8, 1.7, and 1.75-fold, respectively) after 5FU treatment in sorted Mks (FSC^{hi}CD41$^+$) from *Scl-Cre$^-$:Fgfr1$^{fx/fx}$* mice but not from *Scl-Cre$^+$:Fgfr1$^{fx/fx}$* mice (Figure 5F). Furthermore, *Fgf1* and *Fgf2* mRNA levels declined in *Scl-Cre$^+$:Fgfr1$^{fx/fx}$* mice (58% and 42%, respectively) compared with the untreated group (Figure 5F). We further examined FGF1 and FGFR1 levels in the *Fgf2* KO mouse model. Whereas protein levels of FGFR1 and FGF1 in MKs (FSC^{hi}CD41$^+$) after 5FU treatment increased 40% and 1.64-fold,

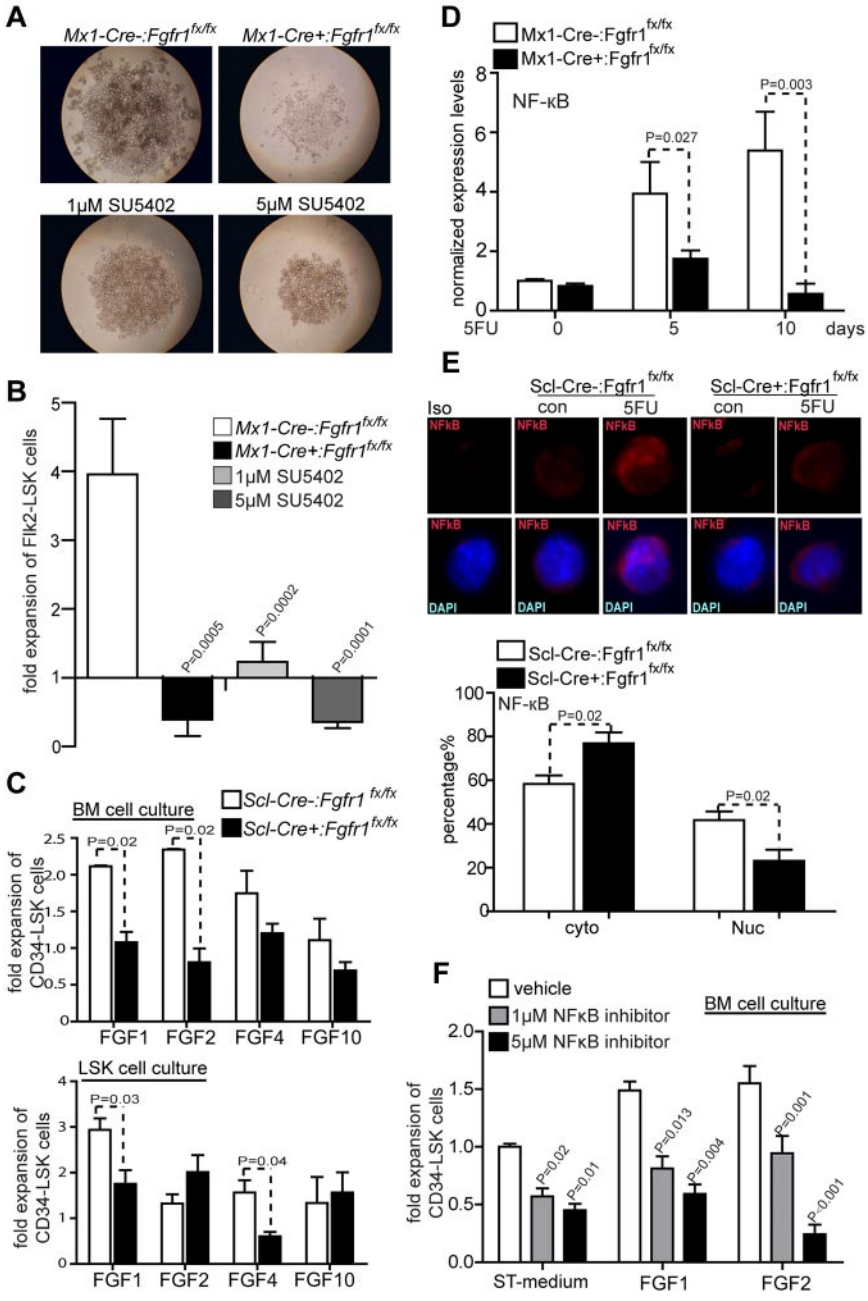

Figure 4. FGF signals facilitate HSPC expansion through FGFR1. (A) BM Flk2$^-$LSK cells from *Mx1*:*Control* or *Mx1*:*CKO* cultured with or without SU5402 14 days. Representative data from 3 independent experiments. (B) Comparison of fold increase of Flk2$^-$LSK cells from *Mx1*:*Control*, *Mx1*:*CKO* and *Mx1*:*Control* plus SU5402 at 1 or 5μM after 14 days culture (n = 6). (C) Comparison of fold increase of CD34$^-$LSK cells from BM cells and sorted LSK cells from *Scl*:*Control* and *Scl*:*CKO* mice, respectively, plus FGF1, 2, 4, or 10 with standard medium after 14 days culture (n = 3). (D) Gene expression analysis of NFκB using qRT-PCR on BM Flk2$^-$LSK cells from *Mx1*:Control, *Mx1*:*CKO* mice on the days indicated after 5FU (n = 3). (E) Representative immunostaining and quantification of subcellular location of NFκB in CD34$^-$LSK cells sorted from *Scl*:*Control* and *Scl*:*CKO* mice. Data pooled from 2 independent experiments. (F) Comparison of fold increase of CD34$^-$LSK cells from BM cells in C57Bl/6 WT mice plus FGF1, FGF2, or with standard medium plus NFκB inhibitor at 1 or 5μM, respectively, as indicated after 14 days culture (n = 4).

respectively, in the control mice, there was no significant increase of FGFR1 and a much lower increase (65.2% less) of FGF1 in MKs (FSC^{hi}CD41$^+$) in *Fgf2* KO mice (Figure 5G-H).

Taken together, these data further confirm that Mks serve as a major resource of FGFs, including FGF1 and FGF2 to support HSPC recovery during BM damage.

FGFR1 inactivation impairs HSPC mobilization induced by BM damage

The reduction of HSPCs in spleen after 5FU treatment (Figure 1D) suggested that FGFR1 may also affect the mobilization of HSPCs. To test this possibility, we monitored numbers of HSPCs in PB by flow cytometry. Under homeostasis, the number of circulating HSPCs is extremely low (Figure 6A). However, 12 days after 5FU, HSPC numbers in PB were substantially increased in control mice. In contrast, the numbers of HSPCs in PB derived from all 3 mouse models, *Mx1-Cre*$^+$*:Fgfr1*$^{fx/fx}$, *Scl-Cre*$^+$*:Fgfr1*$^{fx/fx}$, and *Tek-Cre*$^+$*:Fgfr1*$^{fx/fx}$, were significantly lower (96.9%, 67.5%, and 97.3%, respectively; Figure 6A). Again, we noticed that the absolute numbers of LSK cells were higher in *Mx1-Cre*$^-$*:Fgfr1*$^{fx/fx}$ mice (4.9×10^4 LSKs/mL) than in *Scl-Cre*$^-$*:Fgfr1*$^{fx/fx}$ (1.2×10^4 LSKs/mL) or in *Tek-Cre*$^-$*:Fgfr1*$^{fx/fx}$ (1.16×10^4 LSKs/mL; Figure 6A), which is probably because of the previously mentioned pIpC side effect. Furthermore, we tracked hematopoietic progenitor cell (HPC) mobilization in response to 5FU by measuring changes in the total CFUs. We administered 5FU to *Mx1-Cre*$^-$*:Fgfr1*$^{fx/fx}$ and *Mx1-Cre*$^+$*:Fgfr1*$^{fx/fx}$ mice and performed CFU assays on PB at multiple intervals after treatment. *Mx1-Cre*$^-$*:Fgfr1*$^{fx/fx}$ mice displayed a 3.2-fold greater number of CFUs than did *Mx1-Cre*$^+$*:Fgfr1*$^{fx/fx}$ mice at 14 days after 5FU (Figure 6B). This is consistent

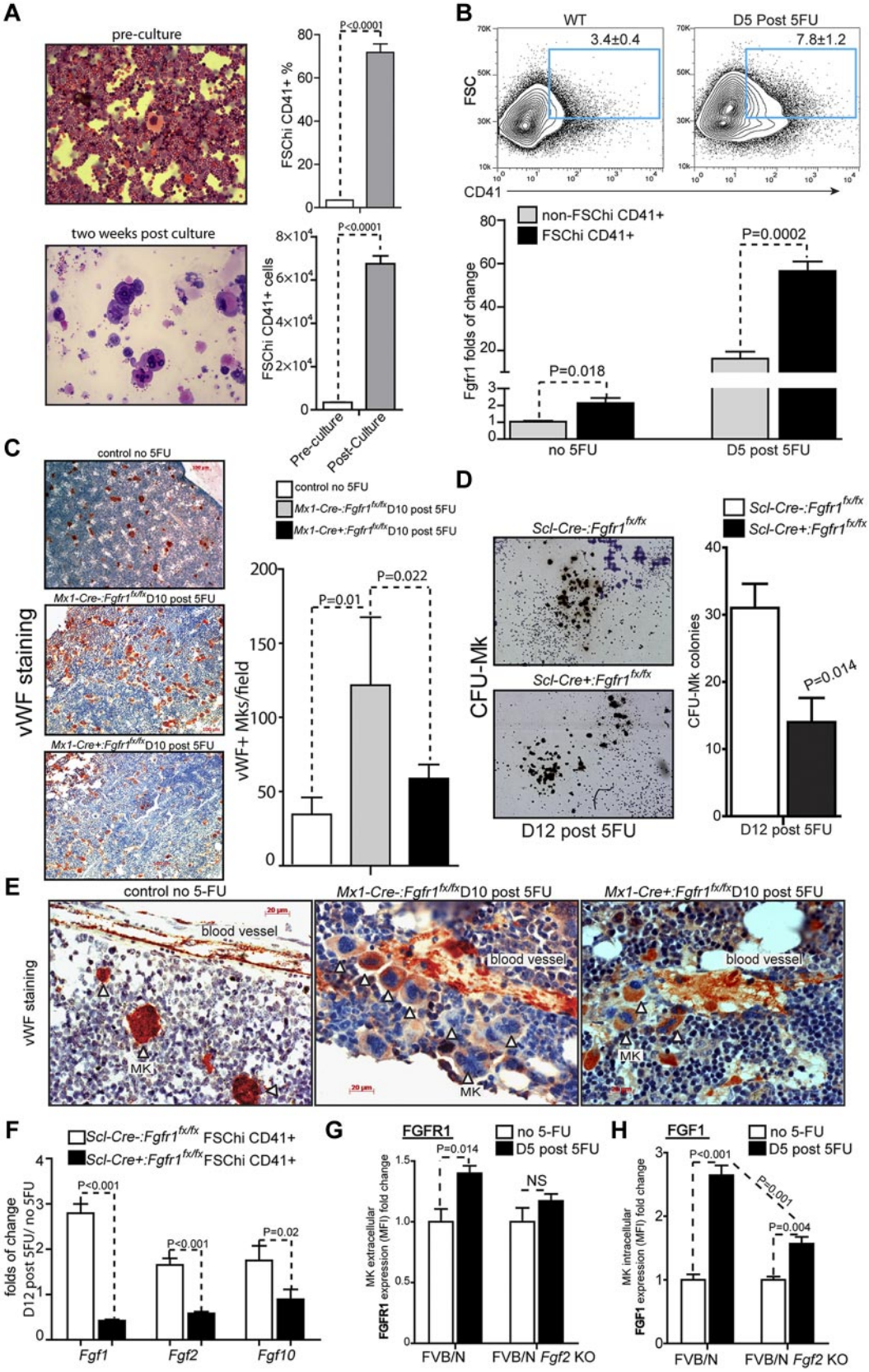

Figure 5. FGFR1 inactivation impairs megakaryocyte proliferation and FGF production induced by BM damage. (A) Cytospin followed by H&E staining and comparison of the frequency and absolute number of FSC^{hi} CD41-positive population in BM cells pre and post–2-week culture (n = 3). (B) Flow cytometric analyses of BM FSC^{hi}CD41^{+} cells and gene expression analysis of *Fgfr1* using qRT-PCR on BM FSC^{hi}CD41^{+} and non-FSC^{hi}CD41^{+} cells from C57Bl/6 WT mice on the days indicated after 5FU (n = 4). (C) Mks stained using VWF (red) and hematoxylin (blue) to label nuclei. Quantification of the numbers of VWF^{+} Mks per field of view from BM and representative BM sections of *Fgfr1 Mx1*:Control, *Mx1:CKO* mice at 10 days after 5FU compared with day 0 (n = 3). (D) Quantification of CFU-Mks and representative CFU-Mk (brown colonies) from *Fgfr1 Scl:Control*, *Scl:CKO* BM at 12 days after 5FU. Representative data from 2 independent experiments. (E) Mks attached to blood vessel stained by VWF at 10 days after 5FU.

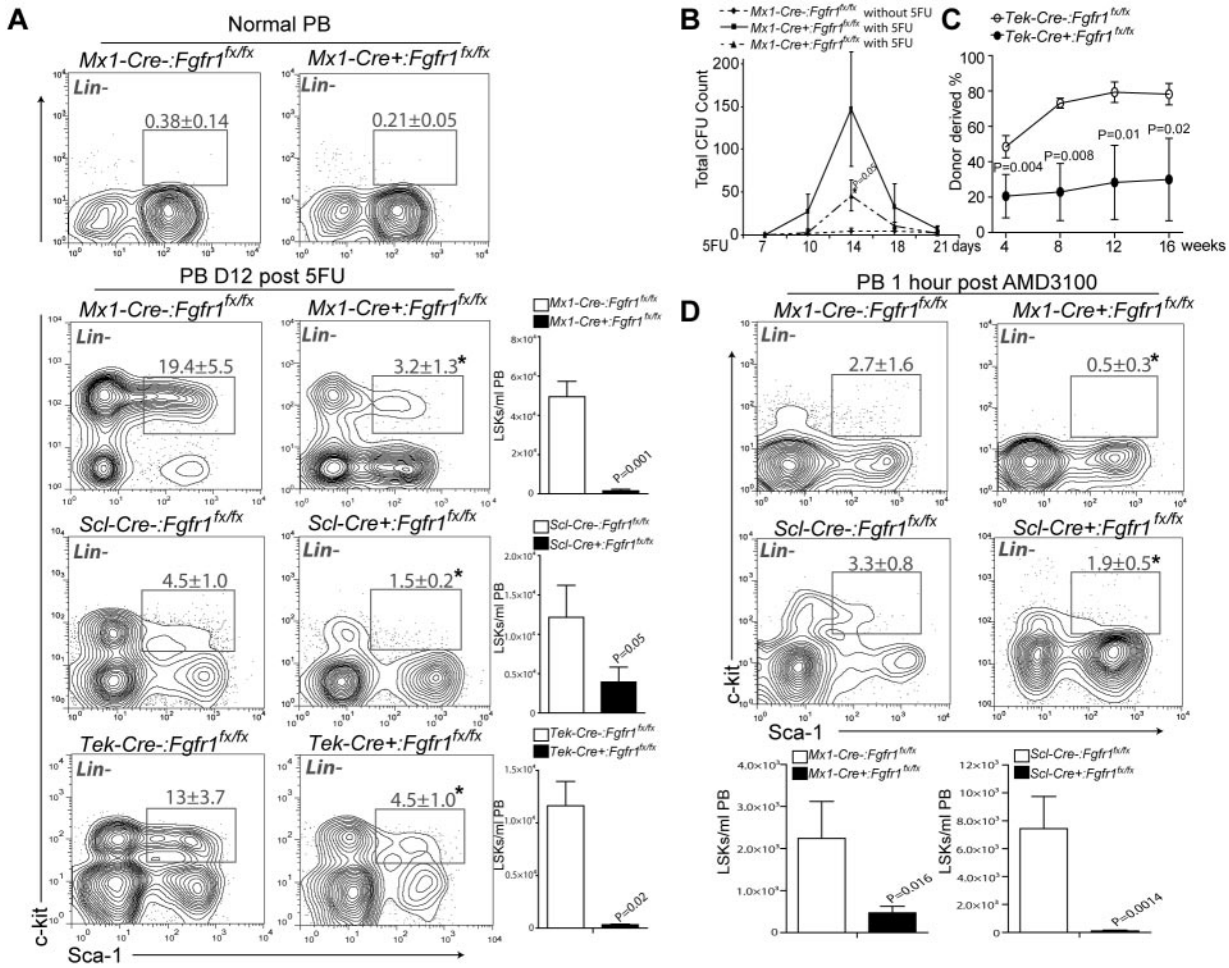

Figure 6. FGFR1 inactivation impairs HSPC mobilization induced by BM damage. (A). Flow cytometric analyses of the LSK population in PB and/or comparison of absolute numbers of LSKs/mL in PB between *Mx1:Control*, *Mx1:CKO* at homeostasis and *Mx1:Control*, *Mx1:CKO* (n = 4), *Scl:Control*, *Scl:CKO* (n = 3), *Tek:Control*, *Tek:CKO* (n = 4) mice 12 days after 5FU. (B) Comparison of total CFUs from PB of *Mx1:Control*, *Mx1:CKO*, mice at 14 days after 5FU (n = 4). (C) PB mononuclear cells 6×10^5) from *Tek:Control*, *Tek:CKO* mice (CD45.2) transplanted 12 days after 5FU together with 2×10^5 rescue BM cells (CD45.1) into lethally irradiated Ptprc recipients PB analysis for total engrafted donor cells at 4, 8, 12, and 16 weeks posttransplantation (n = 5). (D) Flow cytometric analyses of the LSK population in PB and comparison of absolute numbers of LSKs/mL PB between of *Mx1:Control*, *Mx1:CKO*, *Scl:Control*, and *Scl:CKO* mice at 1 hour after AMD3100 treatment (n = 3).

with the report that mobilized HPCs peaked at 14 days after 5FU.[43] According to the kinetics of 5FU-induced mobilization, the time window between day 10 and day 18 is important for HPC mobilization. Next, we performed a repopulation assay to test the functional HSPCs in the *Fgfr1* CKO mice. We transplanted equal numbers of mononuclear cells from PB at 12 days after 5FU from *Tek-Cre*$^-$*:Fgfr1*$^{fx/fx}$ and *Tek-Cre*$^+$*:Fgfr1*$^{fx/fx}$ mice with rescue cells into lethally irradiated recipients. As shown in Figure 6C at 16 weeks after transplantation, PB cells from *Tek-Cre*$^+$*:Fgfr1*$^{fx/fx}$ mice resulted in much lower engraftment (62% less) than those from *Tek-Cre*$^-$*:Fgfr1*$^{fx/fx}$ mice.

The observed reduction in PB HSPCs in *Fgfr1* CKO mice could be because of impaired HSPC migration and/or to impaired HSPC proliferation before BM egress to the bloodstream. To address this issue, we tested whether FGFR1 is required for HSPC mobilization in response to another clinically used mobilizing reagent, an SDF-1 inhibitor AMD3100. AMD3100 acts directly on HSPC-stromal cell interactions and results in rapid HSPC mobilization into the bloodstream.[44] One hour after AMD3100 injection, we observed increased numbers of circulating HSPCs in *Mx1-Cre*$^-$*:Fgfr1* $^{fx/fx}$ and *Scl-Cre*$^-$*:Fgfr1*$^{fx/fx}$ mice, indicating AMD3100-induced HSPC mobilization is independent of prior expansion. HSPC mobilization in *Fgfr1* CKO mice was severely impaired (79.0% and 98.9% fewer absolute LSK cells in *Mx1-Cre*$^+$*:Fgfr1*$^{fx/fx}$ and *Scl-Cre*$^+$*:Fgfr1*$^{fx/fx}$ mice, respectively; Figure 6D). These data show that FGFR1-mediated signaling also promotes HSPC migration, and the rapid mobilization within 1 hour after induction excluded the possibility that HSPC expansion was involved in AMD3100-induced mobilization.

SDF-1 ligand is distributed in gradient in vivo and attracts HSPC migration through its cell surface receptor CXCR4 on HSPCs.[23] Recently it was reported that SDF-1 is increased in PB after AMD3100 treatment, and functional CXCR4 on HSPCs is needed for AMD3100-induced migration.[44] Therefore, we measured the protein level of SDF-1 in PB after 5FU treatment using ELISAs to compare PB supernatants collected from C57Bl/6 mice

Figure 5. (continued) (F) Gene expression analysis of *Fgf1, 2* and *10* using qRT-PCR on BM Mks (FSC^{hi}CD41$^+$ cells) from *Fgfr1 Scl:Control* and *Scl:CKO* mice on the days indicated after 5FU. (G-H) Expression analysis of FGFR1(G) and FGF1(H) using mean fluorescence intensity (MFI) on BM Mks (FSC^{hi}CD41$^+$ cells) from FVB/N WT and FVB/N *Fgf2* KO mice (n = 4).

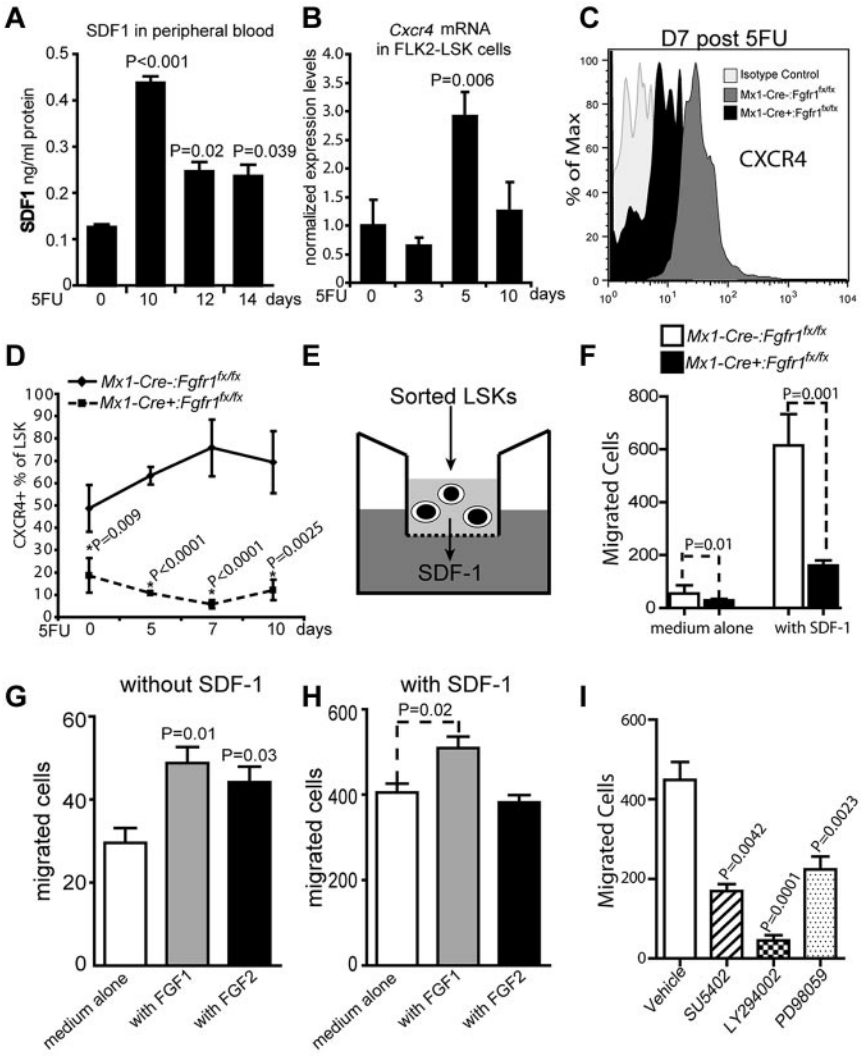

Figure 7. FGFR1 inactivation disrupts SDF-1-CXCR4 pathway for HSPC migration. (A) SDF-1 protein level as determined by ELISA of PB supernatants of C57Bl/6 WT mice on days indicated after 5FU (n = 4). (B) Gene expression analysis of *Cxcr4* using qRT-PCR on BM Flk2$^-$LSK cells from C57Bl/6 WT mice on the days indicated after 5FU (n = 2). (C-D) Timeline of CXCR4 surface expression as a percentage of LSK cells in BM from *Mx1:Control* and *Mx1:CKO* mice after 5FU (n = 3). (E) Illustration of transwell migration assay. (F) Comparison of the chemotactic ability of *Mx1:Control*, and *Mx1:CKO* LSKs (n = 4). (G-H) Comparison of the chemotactic ability of LSKs from C57Bl/6 WT mice plus FGF1, FGF2, or with standard medium (G) without the presence of SDF-1 (n = 3) and (H) with the presence of SDF-1 (n = 3). (I) Comparison of the chemotactic ability of LSKs from C57Bl/6 WT mice in the presence of the following inhibitors: SU5402, LY294002, and PD98059 (n = 6). All results repeated at least 2 times.

at homeostasis and multiple intervals after 5FU. Interestingly, SDF-1 protein level increased 3.5, 2.0, and 1.9-fold at day 10, 12, and 14 after 5FU, respectively (Figure 7A), correlating with the mobilization trend of HSPCs after 5FU (Figure 6B). The increase of SDF-1 level in PB led us to analyze the expression of its receptor, CXCR4, in HSPCs at multiple intervals after 5FU. We found that *Cxcr4* mRNA was up-regulated and peaked at day 5, when HSPCs were expanding within BM and preparing to migrate,[10,45] and then regressed at day 10, when HSPCs were possibly already mobilizing (Figure 7B). Furthermore, we used flow cytometry to compare surface protein levels of CXCR4 on HSPCs from *Fgfr1* CKO and control mice after 5FU. The percentage of CXCR4$^+$LSK cells was 2.6-fold higher in *Mx1-Cre$^-$:Fgfr1$^{fx/fx}$* mice than in *Mx1-Cre$^+$:Fgfr1$^{fx/fx}$* mice at homeostasis, and this difference increased to 12.7-fold at day 7 and 5.8-fold at day 10 after 5FU (Figure 7C-D).

These results led us to predict that HSPCs from *Fgfr1* CKO mice would be defective in their ability to migrate through a microporous membrane in response to the chemotactic signal SDF-1 (Figure 7E).[34] Indeed, in the SDF-1–induced migration assay, HSPCs isolated from *Mx1-Cre$^+$:Fgfr1$^{fx/fx}$* BM showed 2.7-fold fewer migrated cells than from *Mx1-Cre$^-$:Fgfr1$^{fx/fx}$* BM (Figure 7F). To further investigate whether FGF signaling directly facilitates HSPC mobilization, we examined the effects of FGF1 and FGF2 on HSPC migration. We found that adding FGF1or FGF2 led to 65% and 49% increase, respectively, in migrated LSK cells in the medium without SDF-1 (Figure 7G). And FGF1 instead of FGF2 increased migrated LSK cells 26% in the medium containing SDF-1 (Figure 7H). These data indicate that FGF, especially FGF1, may directly facilitate HSPC mobilization. We also studied the effects of different FGFR1 downstream pathways on LSK cell migration from BM of *Mx1-Cre$^-$:Fgfr1$^{fx/fx}$* mice. We found that an FGFR inhibitor (SU5402) reduced the number of LSK cells able to migrate by 2.9-fold; a PI3K inhibitor (LY294002) reduced the number 18.5-fold; and a MEK inhibitor (PD98059) reduced the number 2.1-fold (Figure 7I). These inhibitors did not affect the viability of HSPCs (supplemental Figure 6). As PI3K and MEK are key molecules in the 2 major downstream pathways of the FGF/FGFR signaling complex, these data support our results from FGFR1 inactivation and SU5402-treated LSK cells, and also indicate that FGFR1 signaling is involved in SDF-1–induced chemotaxis. Overall, these results indicate that FGFR1 signaling facilitates mobilization of HSPCs in response to stress.

Discussion

In this study, we used 3 mouse models to inactivate FGFR1. *Mx1-Cre* has a very high recombination efficiency but is not hematopoietic specific and also has a side effect from pIpC that

affected our interpretation of the observed result. *Scl-Cre* is hematopoietic specific; however, incomplete gene deletion resulted in a misleading conclusion regarding a ST versus LT requirement of FGFR1 for HSC engraftment. *Tek-Cre*, mediating a constitutive gene deletion in both hematopoietic and endothelial tissues, has very high gene deletion efficiency. The observation that *Tek-Cre* dependent FGFR1 inactivation did not affect homeostatic hematopoiesis ruled out the possibility of not just intrinsic (HSPC) but also extrinsic (endothelial cells) influences from loss of FGFR1. Transplantation of BM derived from *Fgfr1* CKO mice into wild type recipient mice further tested FGFR1 function when deleted from the hematopoietic system. The experimental results obtained from these models are consistent and complementary in both phenotype and functionality revealed by FGFR1 inactivation. Our results demonstrate that FGFR1-mediated signaling is important for HSPC proliferation and mobilization in vivo in response to BM damage but is not essential under homeostasis. However, we cannot rule out a potential compensation from FGFR3 in homeostasis.

The increase of expression of FGFR1 in HSPCs and their ligands FGF1 and FGF2 in BM after 5FU treatment indicate that FGF pathway activation is part of the hematopoietic stress response. We have shown that FGF signaling, mediated by FGF1 or FGF2 via by FGFR1, is required for both in vitro HSPC expansion and in vivo HSPC proliferation. We further showed that FGF1 may directly and that FGF2 may indirectly regulate HSPC expansion. This observation is consistent with the role of FGF signaling in regulating multiple cellular components and processes to promote survival and growth during cytotoxic stress.[7,8,46]

Regarding the potential source of FGFs in response to BM damage, we observed that Mks after 5FU had increased cell numbers and were enriched in the perivascular region. Because Mks also express CXCR4,[42] the aggregation of Mks is possibly because of the increased SDF-1 level in PB after 5FU treatment (Figure 7A) as suggested by a previous report.[42] Our data indicate that Mks support HSPC recovery by secretion of FGF factors, including FGF1 and FGF2; however FGF production by Mks and expansion of Mks postinjury are severely affected when FGF-FGFR signaling is blocked. Further study is required to investigate the role of Mks in facilitating HSPC proliferation and BM recovery.

Furthermore, the failure of *Fgfr1 CKO* mice to up-regulate NFκB in HSPCs, which is functionally required for HSPC expansion in vitro, partially explains the mechanism of FGFR1 on HSPC expansion, consistent with a previous report that MAPK stimulates NFκB transcription.[47] In addition, AKT has been shown to regulate NFκB activity by controlling its subcellular localization, specifically its nuclear accumulation.[48] NFκB inhibition may have nonspecific effects beyond FGFR signaling; the observation that failure to up-regulate NFkB in response to injury in *Fgfr1* mutant HSPCs still suggests that regulation of NFκB by FGF signaling may play a role in supporting HSPC survival during expansion and mobilization.

In addition to affecting HSPC proliferation, FGFR1 inactivation directly affects HSPC migration from BM to bloodstream as evidenced by the mobilzation defect induced by interruption of SDF-1–CXCR4 interactions via AMD3100.[49] Mechanistically, we found that SDF-1 was increased in PB, and that FGFR1 signaling was required for up-regulation of CXCR4 within HSPCs in response to BM damage, accounting for the diminished responsiveness of FGFR1-null HSPCs to stress-induced changes in SDF-1 gradients.[50] In vitro migration assays (Figure 7I) confirmed that the downstream components of FGF signaling, AKT and MAPK, are involved in FGFR1-facilitated HSPC migration.

In summary, we provide the first in vivo evidence showing that FGFR1-mediated signaling is important for HSPC proliferation and mobilization in response to severe BM damage, though blockage of this pathway does not affect homeostatic hematopoiesis, thus opening a new avenue for improving HSPC mobilization before harvesting in conjunction with AMD3100, and for promoting blood recovery after BM damage.

Acknowledgments

The authors thank Joachim Goethert for *Scl-Cre* mice; Brandy Lewis and Debra Dukes for technical support; Teri Johnson and Nannette Marsh for assistance with immunohistochemistry; Andrew Box and Craig Semerad for assistance with flow cytometry; Leanne Wiedemann, Joan Conaway, Jay Vivian, Patrick Fields, Mike Werle, and members of the Li laboratory for scientific discussion; and Karen Tannen for editing the paper.

This work was funded by the Stowers Institute for Medical Research. J.M.P. is a Fellow of the Leukemia & Lymphoma Society. A.V. is a recipient of an overseas associateship from Department of Biotechnology, Ministry of S&T, Government of India.

Authorship

Contribution: M.Z. and J.T.R. primarily conducted the experiments; T.I. and T.L. conducted ELISA assay for FGF protein measurement; J.M.P. assisted with in vitro HSPC culture; A.V. provided the RNA seq data; J.S.H. assisted with cell sorting; M.J.H. for genotyping; C.-X.D. provided the *Fgfr1* line; X.C.H. helped with training and trouble shooting and performed quantitative RT-PCR; and L.L. directed the overall project.

Conflict-of-interest disclosure: The authors declare no competing financial interests.

Correspondence: Linheng Li, Stowers Institute for Medical Research, 1000 E 50th St, Kansas City, MO 64110; e-mail: lil@stowers.org.

References

1. Eswarakumar VP, Lax I, Schlessinger J. Cellular signaling by fibroblast growth factor receptors. *Cytokine Growth Factor Rev.* 2005;16:139-149.
2. Thisse B, Thisse C. Functions and regulations of fibroblast growth factor signaling during embryonic development. *Dev Biol.* 2005;287(2):390-402.
3. Johnson DE, Williams LT. Structural and functional diversity in the FGF receptor multigene family. *Adv Cancer Res.* 1993;60:1-41.
4. Faloon P, Arentson E, Kazarov A, et al. Basic fibroblast growth factor positively regulates hematopoietic development. *Development.* 2000; 127:1931-1941.
5. Magnusson PU, Ronca R, Dell'Era P, et al. Fibroblast growth factor receptor-1 expression is required for hematopoietic but not endothelial cell development. *Arterioscler Thromb Vasc Biol.* 2005;25(5):944-949.
6. Akashi K, He X, Chen J, et al. Transcriptional accessibility for genes of multiple tissues and hematopoietic lineages is hierarchically controlled during early hematopoiesis. *Blood.* 2003;101(2):383-389.
7. de Haan G, Weersing E, Dontje B, et al. In vitro generation of long-term repopulating hematopoietic stem cells by fibroblast growth factor-1. *Dev Cell.* 2003;4(2):241-251.
8. Yeoh JS, van Os R, Weersing E, et al. Fibroblast growth factor-1 and -2 preserve long-term repopulating ability of hematopoietic stem cells in serum-free cultures. *Stem Cells.* 2006;24(6): 1564-1572.

9. Longley DB, Harkin DP, Johnston PG. 5-fluorouracil: mechanisms of action and clinical strategies. *Nat Rev Cancer.* 2003;3(5):330-338.
10. Lerner C, Harrison DE. 5-Fluorouracil spares hemopoietic stem cells responsible for long-term repopulation. *Exp Hematol.* 1990;18(2):114-118.
11. Lapidot T, Kollet O. The essential roles of the chemokine SDF-1 and its receptor CXCR4 in human stem cell homing and repopulation of transplanted immune-deficient NOD/SCID and NOD/SCID/B2m(null) mice. *Leukemia.* 2002;16(10):1992-2003.
12. Wilson A, Laurenti E, Oser G, et al. Hematopoietic Stem Cells Reversibly Switch from Dormancy to Self-Renewal during Homeostasis and Repair. *Cell.* 2008;135(6):1118-1129.
13. Li L, Clevers H. Coexistence of quiescent and active adult stem cells in mammals. *Science.* 2010;327(5965):542-545.
14. Calvi LM, Adams GB, Weibrecht KW, et al. Osteoblastic cells regulate the haematopoietic stem cell niche. *Nature.* 2003;425:841-846.
15. Zhang J, Niu C, Ye L, et al. Identification of the haematopoietic stem cell niche and control of the niche size. *Nature.* 2003;425:836-841.
16. Kiel MJ, Yilmaz OH, Iwashita T, Terhorst C, Morrison SJ. SLAM family receptors distinguish hematopoietic stem and progenitor cells and reveal endothelial niches for stem cells. *Cell.* 2005;121:1109-1121.
17. Sugiyama T, Kohara H, Noda M, Nagasawa T. Maintenance of the hematopoietic stem cell pool by CXCL12-CXCR4 chemokine signaling in bone marrow stromal cell niches. *Immunity.* 2006;25(6):977-988.
18. Méndez-Ferrer S, Michurina TV, Ferraro F, et al. Mesenchymal and haematopoietic stem cells form a unique bone marrow niche. *Nature.* 2010;466(7308):829-834.
19. Goodman JW, Hodgson GS. Evidence for stem cells in the peripheral blood of mice. *Blood.* 1962;19:702-714.
20. Wright DE, Bowman EP, Wagers AJ, Butcher EC, Weissman IL. Hematopoietic stem cells are uniquely selective in their migratory response to chemokines. *J Exp Med.* 2002;195(9):1145-1154.
21. Cottler-Fox MH, Lapidot T, Petit I, et al. Stem cell mobilization. Hematology / the Education Program of the American Society of Hematology. *Hematology Am Soc Hematol Educ Program.* 2003;2003:419-437.
22. Papayannopoulou T. Current mechanistic scenarios in hematopoietic stem/progenitor cell mobilization. *Blood.* 2004;103(5):1580-1585.
23. Lapidot T, Petit I. Current understanding of stem cell mobilization: the roles of chemokines, proteolytic enzymes, adhesion molecules, cytokines, and stromal cells. *Exp Hematol.* 2002;30(9):973-981.
24. Elias AD, Ayash L, Anderson KC, et al. Mobilization of peripheral blood progenitor cells by chemotherapy and granulocyte-macrophage colony-stimulating factor for hematologic support after high-dose intensification for breast cancer. *Blood.* 1992;79(11):3036-3044.
25. Neben S, Marcus K, Mauch P. Mobilization of hematopoietic stem and progenitor cell subpopulations from the marrow to the blood of mice following cyclophosphamide and/or granulocyte colony-stimulating factor. *Blood.* 1993;81(7):1960-1967.
26. Shen H, Cheng T, Olszak I, et al. CXCR-4 desensitization is associated with tissue localization of hemopoietic progenitor cells. *J Immunol.* 2001;166(8):5027-5033.
27. Broxmeyer HE, Orschell CM, Clapp DW, et al. Rapid mobilization of murine and human hematopoietic stem and progenitor cells with AMD3100, a CXCR4 antagonist. *J Exp Med.* 2005;201(8):1307-1318.
28. Xu X, Qiao W, Li C, Deng CX. Generation of Fgfr1 conditional knockout mice. *Genesis.* 2002;32(2):85-86.
29. Kühn R, Schwenk F, Aguet M, Rajewsky K. Inducible gene targeting in mice. *Science.* 1995;269(5229):1427-1429.
30. Göthert JR, Gustin SE, Hall MA, et al. In vivo fate-tracing studies using the Scl stem cell enhancer: embryonic hematopoietic stem cells significantly contribute to adult hematopoiesis. *Blood.* 2005;105(7):2724-2732.
31. Koni PA, Joshi SK, Temann UA, Olson D, Burkly L, Flavell RA. Conditional vascular cell adhesion molecule 1 deletion in mice: impaired lymphocyte migration to bone marrow. *J Exp Med.* 2001;193(6):741-754.
32. Montero A, Okada Y, Tomita M, et al. Disruption of the fibroblast growth factor-2 gene results in decreased bone mass and bone formation. *J Clin Invest.* 2000;105(8):1085-1093.
33. Haug JS, He XC, Grindley JC, et al. N-cadherin expression level distinguishes reserved versus primed states of hematopoietic stem cells. *Cell Stem Cell.* 2008;2(4):367-379.
34. Zhang J, Grindley JC, Yin T, et al. PTEN maintains haematopoietic stem cells and acts in lineage choice and leukaemia prevention. *Nature.* 2006;441(7092):518-522.
35. Perry JM, He XC, Sugimura R, et al. Cooperation between both Wnt/{beta}-catenin and PTEN/PI3K/Akt signaling promotes primitive hematopoietic stem cell self-renewal and expansion. *Genes Dev.* 2011;25(18):1928-1942.
36. Zhang CC, Kaba M, Ge G, et al. Angiopoietin-like proteins stimulate ex vivo expansion of hematopoietic stem cells. *Nat Med.* 2006;12(2):240-245.
37. Monfils MH, Driscoll I, Kamitakahara H, et al. FGF-2-induced cell proliferation stimulates anatomical, neurophysiological and functional recovery from neonatal motor cortex injury. *Eur J Neurosci.* 2006;24(3):739-749.
38. Berardi AC, Wang A, Levine JD, Lopez P, Scadden DT. Functional isolation and characterization of human hematopoietic stem cells. *Science.* 1995;267(5194):104-108.
39. Essers MA, Offner S, Blanco-Bose WE, et al. IFNalpha activates dormant haematopoietic stem cells in vivo. *Nature.* 2009;458(7240):904-908.
40. Phillips DR, Charo IF, Parise LV, Fitzgerald LA. The platelet membrane glycoprotein IIb-IIIa complex. *Blood.* 1988;71(4):831-843.
41. Dominici M, Rasini V, Bussolari R, et al. Restoration and reversible expansion of the osteoblastic hematopoietic stem cell niche after marrow radioablation. *Blood.* 2009;114(11):2333-2343.
42. Avecilla ST, Hattori K, Heissig B, et al. Chemokine-mediated interaction of hematopoietic progenitors with the bone marrow vascular niche is required for thrombopoiesis. *Nat Med.* 2004;10:64-71.
43. Heissig B, Hattori K, Dias S, et al. Recruitment of stem and progenitor cells from the bone marrow niche requires MMP-9 mediated release of kit-ligand. *Cell.* 2002;109(5):625-637.
44. Dar A, Schajnovitz A, Lapid K, et al. Rapid mobilization of hematopoietic progenitors by AMD3100 and catecholamines is mediated by CXCR4-dependent SDF-1 release from bone marrow stromal cells. *Leukemia.* 2011;25(8):1286-1296.
45. Venezia TA, Merchant AA, Ramos CA, et al. Molecular signatures of proliferation and quiescence in hematopoietic stem cells. *PLoS Biol.* 2004;2(10):e301.
46. Moroni E, Dell'Era P, Rusnati M, Presta M. Fibroblast growth factors and their receptors in hematopoiesis and hematological tumors. *J Hematother Stem Cell Res.* 2002;11(1):19-32.
47. Malinin NL, Boldin MP, Kovalenko AV, Wallach D. MAP3K-related kinase involved in NF-kappaB induction by TNF, CD95 and IL-1. *Nature.* 1997;385(6616):540-544.
48. Dan HC, Cooper MJ, Cogswell PC, Duncan JA, Ting JP, Baldwin AS. Akt-dependent regulation of NF-kappaB is controlled by mTOR and Raptor in association with IKK. *Genes Dev.* 2008;22(11):1490-1500.
49. Rosenkilde MM, Gerlach LO, Jakobsen JS, Skerlj RT, Bridger GJ, Schwartz TW. Molecular mechanism of AMD3100 antagonism in the CXCR4 receptor: transfer of binding site to the CXCR3 receptor. *J Biol Chem.* 2004;279(4):3033-3041.
50. Avecilla ST, Hattori K, Heissig B, et al. Chemokine-mediated interaction of hematopoietic progenitors with the bone marrow vascular niche is required for thrombopoiesis. *Nat Med.* 2004;10(1):64-71.